Available online at www.sciencedirect.com
SCIENCE DIRECT®
Geochimica et Cosmochimica Acta 70 (2006) 267–276
Geochimica
www.elsevier.com/locate/gca

Acid–base activity of live bacteria: Implications for quantifying cell wall charge

Jacqueline Claessens [a,*], Yvonne van Lith [b], Anniet M. Laverman [a], Philippe Van Cappellen [a]

[a] *Utrecht University, Faculty of Geosciences, Department of Earth Sciences, Geochemistry, P.O. Box 80021, 3508 TA Utrecht, The Netherlands*
[b] *Utrecht University, Faculty of Geosciences, Department of Earth Sciences, Stratigraphy and Paleontology, P.O. Box 80021, 3508 TA Utrecht, The Netherlands*

Received 17 May 2005; accepted in revised form 9 September 2005

Abstract

To distinguish the buffering capacity associated with functional groups in the cell wall from that resulting from metabolic processes, base or acid consumption by live and dead cells of the Gram-negative bacterium *Shewanella putrefaciens* was measured in a pH stat system. Live cells exhibited fast consumption of acid (pH 4) or base (pH 7, 8, 9, and 10) during the first few minutes of the experiments. At pH 5.5, no acid or base was required to maintain the initial pH constant. The initial amounts of acid or base consumed by the live cells at pH 4, 8, and 10 were of comparable magnitudes as those neutralized at the same pHs by intact cells killed by exposure to gamma radiation or ethanol. Cells disrupted in a French press required higher amounts of acid or base, due to additional buffering by intracellular constituents. At pH 4, acid neutralization by suspensions of live cells stopped after 50 min, because of loss of viability. In contrast, under neutral and alkaline conditions, base consumption continued for the entire duration of the experiments (5 h). This long-term base neutralization was, at least partly, due to active respiration by the cells, as indicated by the build-up of succinate in solution. Qualitatively, the acid–base activity of live cells of the Gram-positive bacterium *Bacillus subtilis* resembled that of *S. putrefaciens*. The pH-dependent charging of ionizable functional groups in the cell walls of the live bacteria was estimated from the initial amounts of acid or base consumed in the pH stat experiments. From pH 4 to 10, the cell wall charge increased from near-zero values to about -4×10^{-16} mol cell^{-1} and -6.5×10^{-16} mol cell^{-1} for *S. putrefaciens* and *B. subtilis*, respectively. The similar cell wall charging of the two bacterial strains is consistent with the inferred low contribution of lipopolysaccharides to the buffering capacity of the Gram-negative cell wall (of the order of 10%).

1. Introduction

The presence and activity of microorganisms affect the redox state, acid–base properties, and chemical speciation of environmental fluids. Interactions between microorganisms and their immediate surroundings are regulated via the cell wall, across which chemical substances enter and leave the cell. Furthermore, cell walls offer a variety of functional groups that provide binding sites for solute and colloidal species present in the environment. In particular, carboxylate, phosphate, and amino groups have been identified as potential groups affecting the chemical functioning of the cell-water interface (e.g., Haas et al., 2001; Plette et al., 1995; Van der Wal et al., 1997a).

As a result of protonation and deprotonation of functional groups, cell walls exhibit a pH-dependent charge. At most environmental pHs, cell walls of microorganisms, such as bacteria, carry an overall negative surface charge and, therefore, exhibit a high affinity for metal cations (e.g., Agraz et al., 1994; Borrok and Fein, 2005; Daughney et al., 2001; Haas et al., 2001; Kelly et al., 2002; Plette et al., 1996; Urrutia Mera et al., 1992). Metals complexed in the cell wall may serve as nucleation sites for mineral precipitation via counter adsorption of anions (Schultze-Lam et al., 1996).

Because the acid–base behavior of cell walls is crucial to understanding metal binding, cell-mineral adhesion, and

* Corresponding author. Fax: +31 30 2535302.
E-mail address: j.claessens@geo.uu.nl (J. Claessens).

0016-7037/$ - see front matter © 2005 Elsevier Inc. All rights reserved.
doi:10.1016/j.gca.2005.09.006

microbially induced mineralization or dissolution processes, there have been growing efforts to characterize the functional groups in cell walls. Acid–base titrations offer a powerful technique to quantify the protonation and deprotonation of functional groups and they have been used widely to study the mineral-aqueous solution interface (Dzombak and Morel, 1990). Their application, however, has been extended to bacterial cell walls. While titrations were initially carried out mainly with dead bacterial cells or isolated cell walls (Goncalves et al., 1987; Plette et al., 1995; Van der Wal et al., 1997a), a number of recent studies have employed live cells of Gram-positive (Borrok and Fein, 2005; Daughney and Fein, 1998; Daughney et al., 2001) and Gram-negative bacteria (Haas, 2004).

The interpretation of acid–base titrations performed on live cells is not straightforward, however. In a previous study, we have shown that the acid and base consumption of suspensions of live cells of the Gram-negative bacterium *Shewanella putrefaciens* cannot be explained solely as a result of protonation and deprotonation of functional groups (Claessens et al., 2004). Hysteresis of continuous titration curves indicated the occurrence of irreversible processes, most likely related to cellular metabolism and, possibly, to the destabilization of the cell wall. Therefore, rather than performing traditional, continuous titrations, we measured the acid and base consumption of cell suspensions at constant pH, as a function of time (pH stat method).

The present study builds on our previous, preliminary findings. In order to separate the contributions of protonation and deprotonation of functional groups from those of other processes affecting the acid–base behavior of live cells, we performed new series of pH stat experiments with live cells, intact dead cells, and disrupted cells of *S. putrefaciens*. In the experiments with live cells, the solutions were screened for the build-up of products indicative of metabolic activity, especially fatty acids. In addition, we determined the buffering capacity of lipopolysaccharides, a major constituent of the cell wall of Gram-negative bacteria, and we compared the acid–base behavior of *S. putrefaciens* to that of the Gram-positive bacterium *Bacillus subtilis*.

2. Materials and methods

2.1. Bacteria

A Gram-negative bacterium, *S. putrefaciens* strain 200R, and a Gram-positive bacterium, *B. subtilis*, were used. *S. putrefaciens* was originally isolated from crude oil, but its presence has been detected in a variety of aquatic and subsurface environments (Venkateswaran et al., 1999). *B. subtilis* is a common bacterium in soil and vegetation (Pinchuk et al., 2002). Pure cultures of *S. putrefaciens* strain 200R and *B. subtilis* were grown at room temperature in liquid Luria–Bertani (LB) medium. The bacteria were harvested in mid-logarithmic phase and pelletized by centrifugation (5000*g* for 20 min). The supernatant was discarded and the pelletized cells were resuspended in 150 mM NaCl salt solution. The washing procedure was repeated one more time, to obtain the bacterial stock suspensions used in the experiments. Cell densities of the bacterial stock suspensions were derived from the optical densities (OD) measured at 660 nm wavelength on the harvested cultures. The OD-values were calibrated by counting viable cells growing on solid medium and by using the acridine orange direct count (AODC) method (Lovley and Phillips, 1988). The harvested cultures contained of the order of 10^9 cells ml^{-1}.

Cell weights of *S. putrefaciens* and *B. subtilis* were determined by centrifuging pre-concentrated stock suspensions at 5000*g* for 20 min and discarding the supernatant. Wet weights were measured on pellets air-dried at room temperature for 2–3 h, until no visible free water remained. Dry weights were determined on oven-dried pellets (40 °C, 7 h). In contrast to air-drying, the pellet volume noticeably decreased as a result of oven drying. The weights of the pellets were corrected for salt contributions from the medium. Weight determinations were performed on triplicate aliquots; standard deviations were less than 2%. For *S. putrefaciens* air-dried and oven-dried pellets yielded 2×10^{-12} and 7×10^{-13} g $cell^{-1}$, respectively. For *B. subtilis* the corresponding values were 6×10^{-12} and 4×10^{-12} g $cell^{-1}$. The higher and lower densities were considered to be representative of the wet and dry weights of the bacterial cells, respectively.

Intact dead cells of *S. putrefaciens* were prepared by exposing aliquots of the bacterial stock suspension to γ-radiation (25 kGr, Isotron Nederland B.V., Ede) and ethanol (1 h in 50% v/v ethanol). γ-Radiation damage to biological materials results from reactions with radicals produced from ionized water (Greenstock, 1981). In particular, gamma radiation breaks up DNA strands, thereby preventing the cells from replicating. Ethanol kills bacterial cells by denaturating proteins, although it may also partially dissolve membrane lipids (Prescott et al., 1996). After the treatments, the cells were pelletized by centrifugation (5000*g* for 20 min) and resuspended in 150 mM NaCl, and the washing procedure was repeated.

Cells of *S. putrefaciens* were also disrupted in a French press at 8000 psi. The applied pressure causes the intracellular pressure to increase. As the cells are released through the outlet tube, the external pressure drops instantaneously to atmospheric pressure. The pressure differential between the outside and inside of the cells causes them to burst, releasing the intracellular contents. Of the order of 10% of the cells survived the French press treatment and were pelletized by centrifugation (5000*g* for 20 min). The supernatant contained the envelopes and intracellular contents of the disrupted cells. In the following sections, the supernatant is referred to as disrupted cells.

Gram-negative bacteria differ from Gram-positive bacteria by the presence of an outer membrane containing lipopolysaccharides (LPS) (Madigan et al., 1997). As LPS is specific for Gram-negative bacteria, its acid–base proper-

ties were studied separately. Pure LPS (Fluka 62326) from the Gram-negative bacterium, *Escherichia coli*, was dissolved in 150 mM NaCl to a final concentration of 1.203 g L^{-1}.

2.2. pH stat experiments

The acid–base activity and properties of the live and dead cell suspensions, as well as LPS, were measured in a pH stat system (Claessens et al., 2004). The experiments were performed using an automated titrator (Metrohm 716S controlled by Metrohm Tinet 2.4) at 22 °C. The pH of a 150 mM NaCl solution (145 ml) was brought to the desired value of 4, 5.5, 8 or 10 by addition of 0.01 M HCl or 0.01 M NaOH solutions. Equal volumes (5 ml) of cell suspensions (live and dead) or LPS were added to final concentrations of 10^8 cells ml^{-1} or 0.04 g L^{-1} LPS. For suspensions of live cells of *S. putrefaciens*, additional pH stat experiments were carried out at pH 7 and 9. In two more experiments, suspensions of live cells of *S. putrefaciens* were pre-equilibrated at pH 4 for 1.4 h, before adjusting the pH to 8 and 10 by adding NaOH.

The consumption of HCl or NaOH required to keep the pH constant was monitored for periods of up to 5 h. The added titrant volumes were automatically recorded every minute. The total consumption of acid or base was corrected for the consumption by the salt solution alone, to derive the net consumption of protons or hydroxyls by the cells or LPS. The background consumption of acid or base by the salt solution alone was less than 15% of those of the cell suspensions at pH 4 and 8, and less than 20% at pH 10, except for ethanol treated cell suspensions where the background correction at pH 10 reached 30% at the end of the experiment. The pH stat experiments with suspensions of live and ethanol treated cells of *S. putrefaciens* were performed at least in triplicate, and standard deviations were calculated. All other experiments were performed once.

In the experiments at pH 4, 5.5, 8, and 10 with live cells of *S. putrefaciens*, the solutions were analyzed for the presence of fatty acids. At fixed times (0, 1, 2.5, 4, and 5 h) an aliquot of 2.5 ml was collected, filtered through a 0.2 μm pore size filter, and analyzed by Ion Exclusion Chromatography (Dionex DX 120). A column (ICE-AS6) and suppressor (AMMS-ICE II) were used for efficient separation of low molecular weight aliphatic organic acids. The eluent was a 0.4 mM heptafluorobutyric acid solution and the regenerant a 5 mM tetrabutylammoniumhydroxide solution. A standard solution of 1 mM formiate, lactate, acetate, succinate and propionate was prepared and diluted to final concentrations of 5, 10, 30, 50, and 100 μM for calibration. The matrix of the standard solution was 150 mM NaCl to match that of the samples.

2.3. Electrophoretic mobility measurements

The electrophoretic mobility of *S. putrefaciens* cells was measured as a function of pH in 1, 10, and 100 mM NaCl solutions. The pH of the cell suspensions was brought to pH 3.2 with 0.01 M HCl and equilibrated for 30 min. Subsequently, the pH was brought to pH 10 in steps of 0.4 pH units, with a 0.01 M NaOH solution. After each addition of base, the solution was allowed to equilibrate for 20 min. Unfiltered aliquots were directly injected in a Coulter Delsa 440sx and the electrophoretic mobility was measured at two positions in the measuring cell. At each position, the measurement was repeated four times.

3. Results

3.1. Acid–base activity of live cells

In pH stat experiments with live cells of *S. putrefaciens*, no acid or base was needed initially to keep the pH of the bacterial suspension constant at pH 5.5. At pH 4, rapid acid consumption occurred during the first few minutes after adding the cells, followed by more gradual acid consumption, which ended after 50 min (Fig. 1A). Similarly, under neutral and alkaline conditions (pH 7, 8, 9, and 10), base was consumed rapidly during the first few minutes of the experiments. In contrast with the experiments at pH 4, however, no cessation of the long-term base neutralization was observed. This is illustrated in Fig. 1A, which shows ongoing base neutralization after 5 h in the pH stat

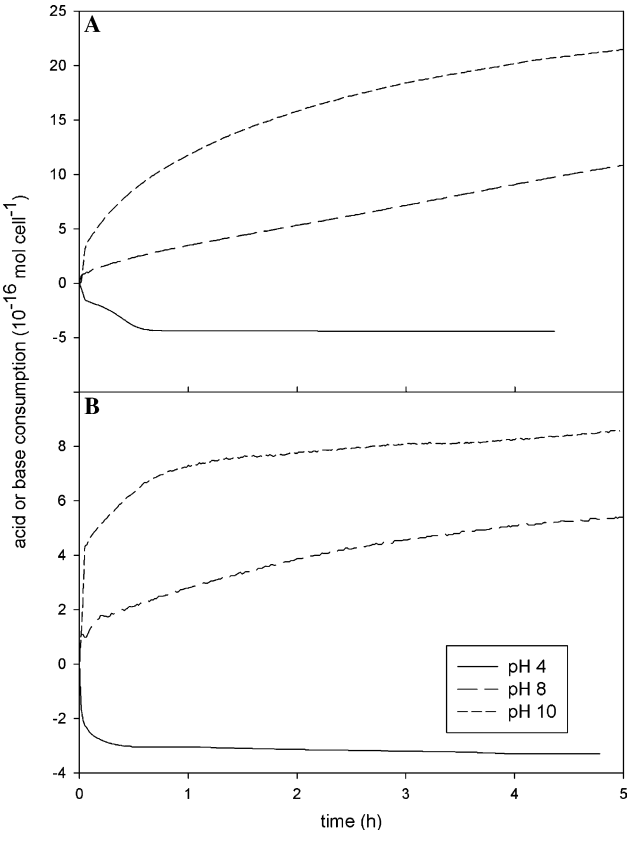

Fig. 1. Acid and base consumption of live cells of *S. putrefaciens* (A) and *B. subtilis* (B) as a function of time at pH 4, 8, and 10, in 150 mM NaCl, at a cell density of 10^8 cells ml^{-1} and a temperature of 22 °C.

experiments at pH 8 and 10. Net base neutralization by suspensions of live *S. putrefaciens* cells measured after 5 h increased systematically from pH 7 to 10. A small upward pH drift (0.13×10^{-16} mol cell^{-1} h^{-1}) also indicated some long-term acid consumption by the cell suspensions at pH 5.5.

The initial amounts of acid or base consumed by the bacterial suspensions were estimated by extrapolating the slow neutralization trends back to time zero, as shown in Fig. 2. These estimates were quite reproducible. Standard deviations of the initial amounts of acid and base consumed by the suspensions of live cells of *S. putrefaciens* did not exceed 17% (Table 1). The amounts of acid and base consumed after five hours had even lower standard deviations of 5%, except at pH 10 where the standard deviations of the long-term (5 h) base consumption were around 15%.

Acid or base consumption curves by suspensions of live cells of *B. subtilis* exhibited features similar to those observed for *S. putrefaciens* (Fig. 1B). No acid or base was consumed when cells were added to pH 5.5 solutions. At pH 4, acid consumption lasted for about 20–30 min, beyond which no further acid addition was required to keep the pH constant. At pH 8 and 10, fast base consumption during the first few minutes was followed by slower, continuous base consumption for the remainder of the experiments. While the initial acid and base consumption per cell was higher for *B. subtilis* than for *S. putrefaciens* (Table 1), after 5 h, base consumption at pH 8 and 10 was significantly lower for the cell suspensions of *B. subtilis*.

The base consumption of live cell suspensions of *S. putrefaciens* at pH 8 and 10 differed significantly whether or not the suspensions had been pre-equilibrated at pH 4 (compare Figs. 1A and 3). After exposing the cells to pH 4 for 1.4 h, base addition during about 15 min was needed to change the pH of the suspensions to 8 or 10. For the remainder of the experiments, however, base consumption was much smaller than in the experiments with no pre-equilibration at pH 4.

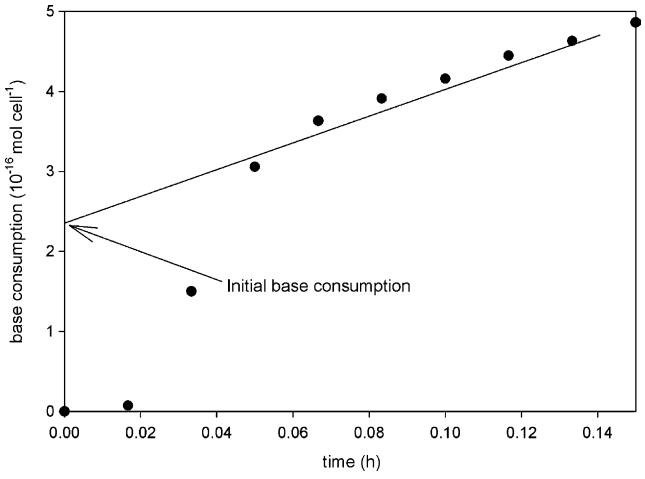

Fig. 2. Example of the determination of initial base consumption by live cells of *S. putrefaciens* at pH 10.

Table 1
Initial acid (pH 4) or base (pH 8 and 10) consumption of live cells of *S. putrefaciens* (Sp) and *B. subtilis* (Bs), dead but intact cells of Sp, disrupted cells of Sp, and lipopolysaccharides (LPS) isolated from *E. coli* expressed in units of 10^{-16} mol cell^{-1}

Cell suspensions	pH 4	pH 8	pH 10
Live cells (Sp)	1.3 ± 0.13	0.7 ± 0.07	2.3 ± 0.40
Live cells (Bs)	2.0	1.4	4.1
Gamma radiated cells	2.8	1.8	2.6
Ethanol treated cells	2.7 ± 0.54	1.1 ± 0.22	1.7 ± 0.68
French press disrupted cells	6.7	3.5	13.7
LPS	0.1	0.1	0.3

3.2. Acid and base buffering by dead cells and LPS

The acid or base activities of dead cells of *S. putrefaciens* in pH stat experiments were fundamentally different from those observed for the live cells, as shown in Figs. 4A–C, for pH 4, 8, and 10, respectively. Rapid consumption of acid or base in suspensions of dead cells lasted a few minutes, and then ceased, or proceeded at a very slow rate. In Table 1, the initial acid (pH 4) or base (pH 8 and 10) consumption of the dead cells is compared to the initial acid or base consumption of live cells of *S. putrefaciens* and *B. subtilis*. The initial values listed in the table were determined by extrapolating the long-term buffering trends back to time zero (Fig. 2). This correction mainly affected the estimated initial acid or base consumption by the live cells, however.

The amounts of acid or base consumed by gamma radiated and ethanol treated cells of *S. putrefaciens* were of comparable magnitude, although base consumption at pH 8 and 10 tended to be higher for cells killed by γ-radiation (Figs. 4B and C). Cells disrupted by the French press treatment exhibited systematically much higher acid and

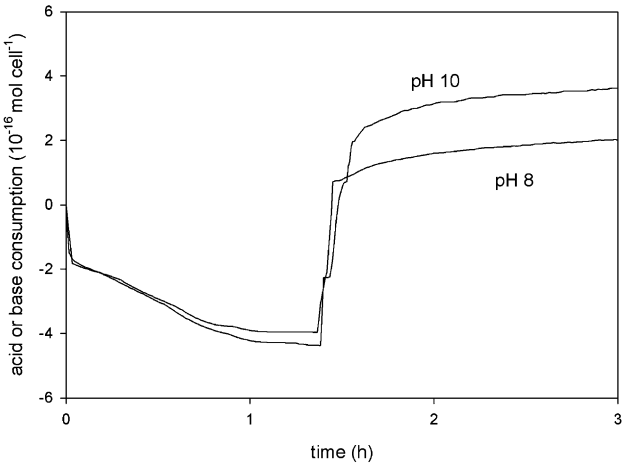

Fig. 3. Acid and base consumption of live cells of *S. putrefaciens* exposed first to a constant pH of 4 for 1.4 h and then to a constant pH of 8 or 10. Experiments are conducted in 150 mM NaCl, at a cell density of 10^8 cells ml^{-1} and a temperature of 22 °C.

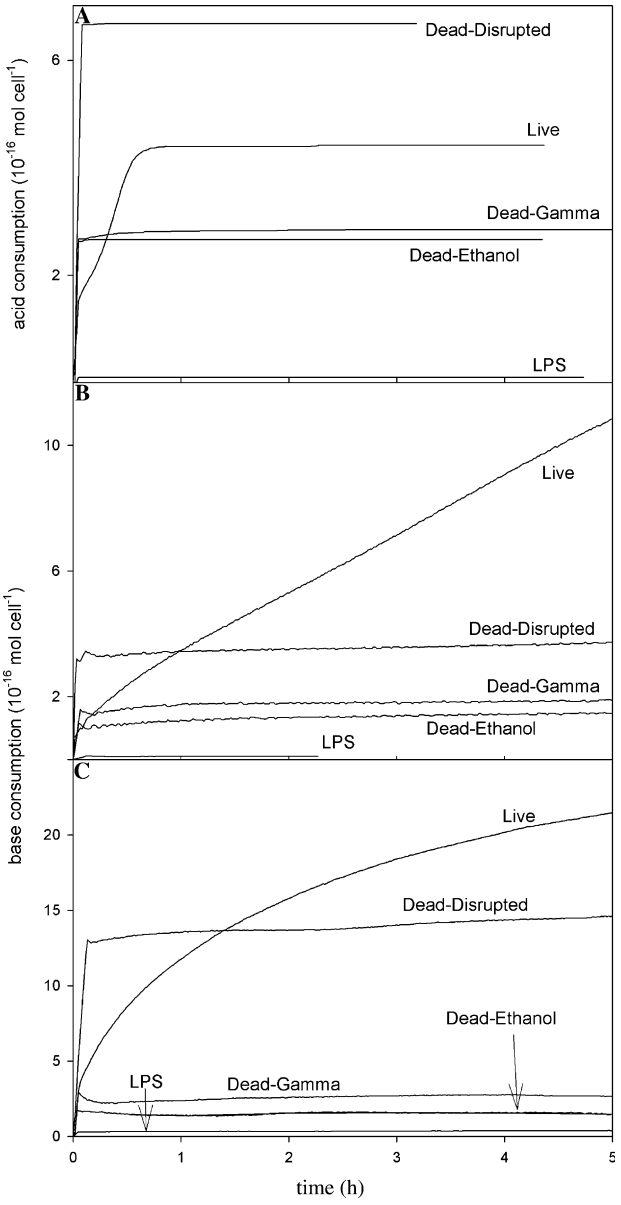

Fig. 4. Acid and base consumption of live cells, dead cells, disrupted cells of *S. putrefaciens*, and LPS as a function of time at pH 4 (A), 8 (B), and 10 (C) in 150 mM NaCl, at a cell density of 10^8 cells ml^{-1} or 0.04 g L^{-1} LPS and 22 °C.

base consumption than dead, but intact, cells. The initial amounts of acid or base consumed by live cell suspensions were comparable, within a factor of 3, to those of the intact dead cells. The reproducibility of initial acid and base consumption in the replicate experiments with ethanol-killed cells, however, was not as good as for live cells, as can be inferred from the standard deviations in Table 1.

At pH 4, acid consumption by the live cells of *S. putrefaciens* reached values intermediate between those of intact dead cells and disrupted cells (Fig. 4A). At pH 8 and 10, base consumption at the end of the experiments was significantly higher for the live than for the dead cells (Figs. 4B and C). These results further highlight the very different buffering behavior of *S. putrefaciens* under acidic and basic conditions.

To estimate the potential contribution of lipopolysaccharides to the acid–base buffering capacity of cell walls of Gram-negative bacteria, the acid or base consumption measured in the LPS suspensions was expressed on a per cell basis (Table 1, Figs. 4A–C). The calculations assumed that the dry weight of *S. putrefaciens* cells is 7×10^{-13} g $cell^{-1}$ (Section 2.1) and that LPS accounts for 3.4% of the dry weight of Gram-negative bacteria (Madigan et al., 1997). According to the results, LPS may, at most, account for 10% of the buffering capacity of the Gram-negative cell wall.

3.3. Fatty acid production

Lactate and propionate were not detected in the filtered solutions of the pH stat experiments with live cells of *S. putrefaciens*. Measurable levels of acetate (5 µmol L^{-1}) and formiate (10 µmol L^{-1}) were found at pH 4, 5.5, 8, and 10, but no clear trends with time were observed. Solutions of the experiments at pH 8 and 10 additionally contained succinate. In the case of succinate, however, the concentrations systematically increased with time (Fig. 5). The build-up of succinate was higher at pH 10 than at pH 8.

3.4. Electrophoretic mobility

The isoelectric point (iep) of live cell suspensions of *S. putrefaciens* fell between pH 3.5 and 4, for the three electrolyte concentrations used (Fig. 6). With increasing pH, the electrophoretic mobility increased, consistent with the development of pH-dependent negative charge on the cells. The increase in electrophoretic mobility was more pronounced in 1 and 10 mM NaCl than in 100 mM NaCl. In 100 mM NaCl solution, the electrophoretic mobility remained constant above pH 7, while in 1 and 10 mM NaCl solutions it continued to increase slowly until pH 10.

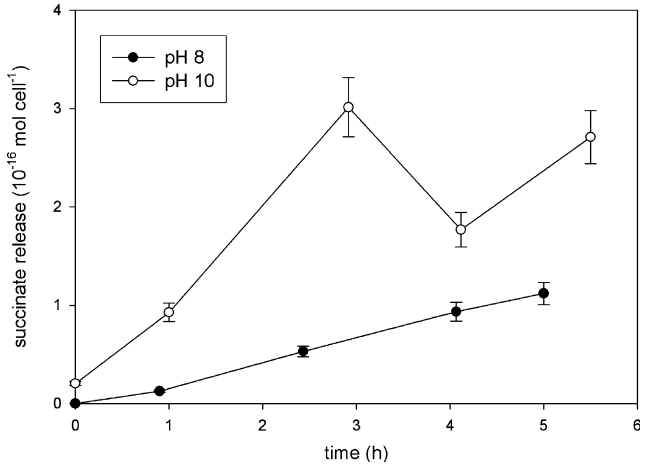

Fig. 5. Release of succinate by live cells of *S. putrefaciens* as a function of time at pH 8 and 10, in 150 mM NaCl, at a cell density of 10^8 cells ml^{-1} and 22 °C.

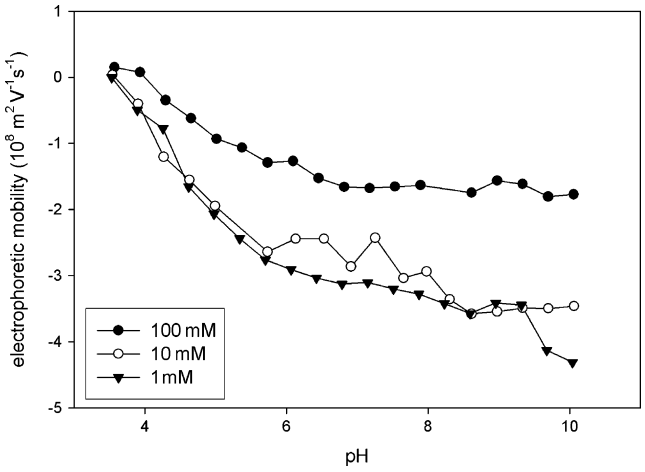

Fig. 6. Electrophoretic mobility of cells of *S. putrefaciens* as a function of pH in 1, 10, and 100 mM NaCl.

4. Discussion

4.1. Acid–base activity of bacterial cells

The acid and base consumption of live cells of *S. putrefaciens* differs greatly from that of dead cells (Figs. 4A–C). Dead cells exhibit little or no acid–base activity beyond the first few minutes of exposure to new pH conditions. The fast acid or base consumption by the dead cells most likely reflects the buffering capacity of the cell wall and, in the case of disrupted cells, also the intracellular content. Consequently, disrupted cells yield higher acid or base neutralization than dead, but intact, cells (Table 1). The lack of long-term buffering by the intact dead cells argues against a significant leakage of protons across their cytoplasmic membranes.

Physiologically active cells of *S. putrefaciens* also exhibit fast acid or base consumption during the first few minutes of the pH stat experiments. The initial amounts of acid or base neutralized are of similar magnitude for live and intact dead cells, although some significant differences are observed (Table 1). At pH 8 and 10, the differences in initial buffering capacity between γ-radiated and ethanol treated cells, however, are of the same order of magnitude as those observed between live and dead bacteria. Furthermore, the replicate experiments with ethanol treated cells show a large variability, suggesting that the ethanol treatment creates artifacts in the cell wall buffering capacity.

Exposure of bacterial cells to ethanol causes denaturation of proteins and may dissolve membrane lipids (Prescott et al., 1996), while hydroxyl and superoxide radicals oxidize cell wall lipids and proteins during gamma radiation. In the latter case, the oxidative stress results in a reorganization of the fatty acid pattern and may alter the secondary structure of proteins (Benderitter et al., 2003). These various physical-chemical changes of the cell wall are likely to affect its acid–base properties. Therefore, we consider the initial acid or base consumption by the live cells to be the more accurate measure of the protonation or deprotonation of functional groups in the unaltered cell wall.

Viable cell counts show that *S. putrefaciens* cells die upon exposure to pH 4 (Claessens et al., 2004), which is consistent with the cessation of acid neutralization after 50 min observed at pH 4 (Fig. 4A), and with the much reduced base neutralization at pH 8 and 10 by cells pre-equilibrated at pH 4 (Fig. 3). The initial fast acid consumption in the pH stat experiments at pH 4 is not immediately followed by cessation of all acid neutralization activity, however (Fig. 4A). At pH 4, the cell suspensions continue to neutralize acid at near-constant rate for about 50 min. Possibly, protons are pumped into the cell, where they are neutralized by the intracellular buffering capacity. Van der Wal et al. (1997a) similarly invoked proton transport across the cytoplasmic membrane to explain the hysteresis of continuous acid–base titration curves of whole live cells of a Gram-positive bacterium. Comparison of acid consumption by live and disrupted cells (Fig. 4A) indicates that the intracellular buffering capacity is sufficient to explain proton consumption beyond the fast initial acid buffering.

At pH 7 and higher, the evidence points to an additional mechanism of base neutralization. As shown in Figs. 4B and C, base consumption by live cells of *S. putrefaciens* at pH 8 and 10 clearly exceeds that of disrupted cells. Therefore, the buffering capacities of cell wall and intracellular content together cannot account for the observed long-term (>1 h) buffering. Aerobic respiration is the likely source of the long-term base neutralization, as indicated by the measurable build-up of succinate in the suspensions at pH 8 and 10 (Fig. 5). Succinate is one of the intermediate products of the tricarboxylic acid cycle (Madigan et al., 1997). During respiration, cells convert their intracellular sugar reserves, e.g. glucose, into pyruvate (glycolysis). Pyruvate is a substrate for the tricarboxylic acid cycle, and its transformation produces succinate and releases CO_2. The acidity associated with CO_2 is then transferred to the extracellular solution, directly as CO_2 or as protons via the proton-motive force across the cell membrane.

Interestingly, the intensity of long-term base neutralization by live cells of *S. putrefaciens* seems to be directly related to the pH of the surrounding medium. From pH 7 on, the net amount of base neutralization measured after 5 h increases systematically with pH. We hypothesize that the cells adjust their respiration rate to the surrounding pH: the more the pH exceeds the optimal growth pH (7.0), the higher the respiratory activity and, hence, the larger the corresponding base neutralization. Obviously, the long-term base buffering in the pH stat experiments is limited by the intracellular reserves of carbon substrates for respiration. Substrate limitation may be responsible for the progressive slowing down of base neutralization observed at pH 10 (Fig. 1A).

Qualitatively, the acid and base consumption curves by live cells of the Gram-positive bacterium *B. subtilis* resemble those of the live cells of *S. putrefaciens*. A closer look at

Table 2
The rate of proton release by live cells of *S. putrefaciens* (Sp) and *B. subtilis* (Bs) expressed in units of 10^{-16} mol cell^{-1} h^{-1} at pH 4, 5.5, 7, 8, 9, and 10 and 22 °C in 150 mM NaCl and 10^8 cells ml^{-1}

pH	Intracellular buffering		Metabolic buffering	
	Sp	Bs	Sp	Bs
4	−2.70	−2.31	0	−0.07
5.5	0	—	−0.13	—
7	2.17	—	0.84	—
8	3.80	3.14	1.87	0.67
9	5.68	—	—	—
10	9.45	4.98	2.79	0.25

The rate of proton release due to intracellular and metabolic buffering was calculated from the amounts of protons released in the pH stat experiments between, respectively, 3 and 18 min and 1.5–4 h.

Figs. 1A and B reveals some important differences, however. For instance, the initial amounts of acid and base consumed indicate that the cells of *B. subtilis* carry more functional groups than *S. putrefaciens* (Table 1). In contrast, the additional amounts of acid and base consumed are significantly lower for *B. subtilis*, implying a reduced intracellular acid buffering capacity and less long-term base neutralization by respiration, compared to *S. putrefaciens*. This is also illustrated in Table 2, where rates of proton release associated with intracellular buffering and respiration are systematically lower for *B. subtilis*.

The results discussed in this section highlight the large variability in acid–base activity of bacterial cells that may be caused by (1) variations in cell wall properties and the initial metabolic state resulting from cell preparation, (2) pH-dependent variations in cell viability and metabolic activity, and (3) inherent differences in cell wall and metabolism among bacterial species. The implications of these and other (e.g., cell wall destabilization, Claessens et al., 2004) sources of variability in acid–base activity for the determination of the cell wall charge associated with the reversible protonation and deprotonation of functional groups are explored further in the next section.

4.2. Cell wall charge

A number of different methods have been used to determine charge development in bacterial cell walls and characterize the responsible functional groups. The most common methods involve continuous acid–base titrations of dead cells (Goncalves et al., 1987), live cells (Daughney and Fein, 1998; Daughney et al., 2001; Haas, 2004), and isolated cell walls (Plette et al., 1995; Van der Wal et al., 1997a). The treatments used to kill the cells, by radiation or chemical agents, or to isolate the cell walls may cause chemical modifications that affect the results of the titrations, as illustrated by the differences in the acid and base consumption curves of *S. putrefaciens* cells treated with γ-radiation and ethanol (see Section 4.1). Continuous titration curves of live cells may be affected by proton consumption or production linked to active cellular processes or cell wall destabilization (Claessens et al., 2004; this study). For example, in continuous titrations of viable cells of *Rhodococcus erythropolis*, Van der Wal et al. (1997a) observed that decreasing the rate of titration increased hysteresis, clearly indicating a contribution from irreversible processes to acid and base neutralization.

The pH stat method used here represents an alternative approach to estimate cell wall charging due to protonation and deprotonation of functional groups of macromolecules present in the unaltered cell wall of live bacteria. In addition, it provides insight into the potential influence of irreversible processes during continuous titrations of cells. For instance, comparison of the time-dependent acid and base consumption by live cells of *S. putrefaciens* and *B. subtilis* indicates that the relative contribution of irreversible processes is larger in the case of *S. putrefaciens* (Figs. 1A, B and Table 2). Therefore, under otherwise identical experimental conditions, continuous titrations of *S. putrefaciens* should exhibit more pronounced hysteresis than titrations of *B. subtilis*.

The results of the pH stat experiments also imply that continuous titration curves should depend on the direction of titration, because cell viability is differently affected by exposure to low and high pH (section 4.1). For the two bacterial species considered in this study, cellular activity should have less impact if live cell suspensions are first titrated acidimetrically, e.g. to pH 4, and then alkalimetrically, e.g. to pH 10. By first exposing the bacteria to acidic conditions, loss of viability should minimize the effects of metabolism during the remainder of the titration, as clearly shown by Fig. 3. The opposite would be true if the cells were first titrated to pH 10 and then to pH 4.

From the initial amounts of acid and base consumed at pH 4 and 10 (Table 1) it is possible to calculate the concentrations of ionizable functional groups within the experimental pH range. The estimated concentrations are 4.0×10^{-16} mol cell^{-1} for *S. putrefaciens* and 6.5×10^{-16} mol cell^{-1} for *B. subtilis* (units are in mol H^+ equivalents). These concentrations are minimum estimates of the total concentrations of ionizable functional groups in the cell walls, because all groups are not necessarily (de)protonated in the pH range 4–10.

Cell wall charges of live cells of *S. putrefaciens* as a function of pH can be calculated from the initial amounts of acid and base consumed, by assuming that the point of zero charge (pzc) coincides with the measured isoelectric point of the cells (iep = 3.75, Fig. 6). The results are shown in Fig. 7 (full symbols). For comparison, the cell wall charges inferred for live cells of *B. subtilis* are also shown, assuming the same pzc (Fig. 7, open symbols), although recent evidence suggests that the pzc of *B. subtilis* may be lower than 3.75 (Fein et al., 2005).

For complex macromolecular structures such as cell walls, the assumption that the pzc and iep are equal is questionable. For example, Gelabert et al. (2004) recently showed that the pzc of diatom cells may be several pH units higher than their iep. They interpret these large differences in terms of the spatial disposition of functional groups

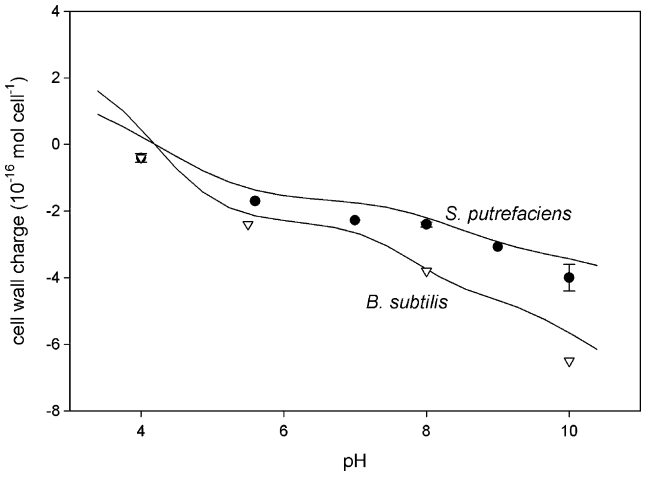

Fig. 7. Cell wall charge of live cells of *S. putrefaciens* and *B. subtilis* as a function of pH in 150 mM NaCl, at a cell density of 10^8 cells ml^{-1} and 22 °C. The symbols correspond to cell wall charges calculated from the initial acid or base consumptions in the pH stat experiments (Table 1), assuming a pzc of 3.75. The continuous curves are cell wall charges predicted using a three-site model comprised of carboxylate (p$K = 4.3$), phosphate (p$K = 7.8$) and amino (p$K = 9.9$) groups. The three sites are assumed to be present in 2:1:1 proportions. The constant capacitance model is used to correct for electrostatic effects, assuming a capacitance of 5F m^{-2}, and specific surface areas of 55 m^2 g^{-1} for *S. putrefaciens* (Haas et al., 2001) and 140 m^2 g^{-1} for *B. subtilis* (Fein et al., 1997). See text for detailed discussion.

within the three-dimensional cell wall structure. Much smaller differences are reported by Van der Wal et al. (1997a) for bacterial cell walls, with pzc values typically about 0.5 units higher than the corresponding iep values. A similar difference would produce a pzc for *S. putrefaciens* of the order of 4.25, causing a small upward shift of the cell wall charges plotted in Fig. 7.

Often the concentrations of functional groups are reported per unit mass bacteria (Daughney and Fein, 1998; Daughney et al., 2001; Haas, 2004), although one also finds concentrations expressed per unit mass or surface area of cell wall (Haas et al., 2001; Van der Wal et al., 1997a). Here, we opt to express the concentrations per cell. The cell is the basic physiological unit, and normalization to cell numbers is common when expressing microbial rates. Comparison of the functional group concentrations determined here with those in other studies, however, is hindered by the uncertainties and methodological biases associated with the determination of cell (or cell wall) masses. This is illustrated in Table 3 where concentrations of ionizable functional groups from a number of studies are converted into cell-normalized values, using the originally reported cell (or cell wall) masses and those obtained here.

For example, for the Gram-positive bacterium *Rhodococcus opacus*, the total concentration of ionizable groups reported by Van der Wal et al. (1997a) is 0.7 mmol g^{-1} cell wall. This bacterium is of similar shape as *S. putrefaciens*, although somewhat larger. Its iep is 3.4, and it exhibits very similar dependencies of the electrophoretic mobility on pH and electrolyte concentration as *S. putrefaciens* (Van der Wal et al., 1997b). If we assume that *S. putrefaciens* cells have the same cell wall density of functional groups (0.7 mmol g^{-1} cell wall) and the same cell wall to cell mass ratio (29%) as *R. opacus*, then, using a wet cell mass of 2×10^{-12} g cell^{-1} (Section 2.1), we obtain a concentration of functional groups of 4.0×10^{-16} mol cell^{-1} (Table 3), which matches the estimate given above. This apparent agreement, however, hinges on the validity of the assumptions made.

Table 3
Cell wall functional group densities

Bacterium	Reported value	Conversion	Concentration in 10^{-16} mol cell^{-1}
R. opacus[a] (Gram+)	0.7 mmol g^{-1} cell wall	2×10^{-12} g cell^{-1}[e] 0.29 g cell wall g^{-1} cell[a]	4
B. subtilis[d] (Gram+)	0.3 mmol g^{-1} cell	2.5 g L^{-1} $\equiv 10^{10}$ cells ml^{-1}[d]	0.75
		6×10^{-12} g cell^{-1}[e]	18
S. putrefaciens[b] (Gram−)	0.14 mmol g^{-1} cell	1.3×10^{-13} g cell^{-1}[b]	0.18
		2×10^{-12} g cell^{-1}[e]	2.7
S. putrefaciens[c] (Gram−)	1.77 μmol mg^{-1} cell	2×10^{-12} g cell^{-1}[e]	35

[a] Van der Wal et al. (1997a).
[b] Haas (2004).
[c] Sokolov et al. (2001).
[d] Daughney and Fein (1998).
[e] This study.

In contrast, based on fitting continuous titration curves of live cells of the same strain of aerobically grown *S. putrefaciens* as used here, Haas (2004) derived a total functional group concentration of 0.14 mmol g^{-1} bacteria. Using the (wet) cell mass reported by this author, 1.3×10^{-13} g cell^{-1} yields a concentration of 0.18×10^{-16} mol cell^{-1} (Table 3), that is, a value significantly lower than that found here. The discrepancy, however, seems to be mostly related to the large difference in cell mass between the two studies. If we use the wet cell mass measured here, 2×10^{-12} g cell^{-1} (section 2.1), the corresponding functional group density is 2.7×10^{-16} mol cell^{-1} (Table 3), which is of the same order of magnitude as that derived from the pH stat experiments. A mass of the order of 10^{-12} g cell^{-1} is more in line with cell weights of *S. putrefaciens* determined by DiChristina (1989). However, combining a cell mass of 2×10^{-12} g cell^{-1} with the functional group concentration of Sokolov et al. (2001) yields a much higher cell-normalized functional group concentration of 35×10^{-16} mol cell^{-1} (Table 3).

Daughney and Fein (1998) performed acid–base titrations on live cells of *B. subtilis* and obtained functional group concentrations of the order of 0.3 mmol g^{-1}. Together with the wet cell mass determined here, 6×10^{-12} g cell^{-1} (Section 2.1), this equals a concentration of 18×10^{-16} mol cell^{-1} (Table 3). According to Fein et al. (1997), however, 2.5 g L^{-1} of *B. subtilis* cells corresponds to 10^{10} cells ml^{-1} and, hence, the functional group concentra-

tion should only be 0.75×10^{-16} mol cell^{-1} (Table 3). The value derived from the pH stat experiments (6.5×10^{-16} mol cell^{-1}) falls somewhere in between these two extremes.

For both bacterial species, the cell wall charge dependence on pH (Fig. 7) shows the characteristic sigmoidal shape that is also observed in continuous titrations of whole cells and isolated cell walls (e.g., Daughney and Fein, 1998; Van der Wal et al., 1997a). The shape is attributed to the existence of weak acid and base groups in the cell wall, whose distinct dissociation constants (p*K*s) give rise to the inflection points of the cell wall charge versus pH curve. Equilibrium models that include a limited number (2–5) of discrete functional groups successfully capture this behavior (e.g., Cox et al., 1999; Daughney and Fein, 1998; Fein et al., 1997; Haas et al., 2001; Plette et al., 1995; Sokolov et al., 2001).

Carboxylate, phosphate, and amino groups are commonly invoked to explain cell wall charging of both Gram-positive and Gram-negative bacteria, although in some models the positively ionizing amino groups are replaced by negatively ionizing hydroxyl groups (e.g., Daughney and Fein, 1998; Fein et al., 1997; Haas, 2004). Inclusion of amino groups allows for the development of a net positive cell wall charge at sufficiently low pH. Models that exclusively include negatively ionizing functional groups (e.g., carboxylate, phosphate, and hydroxyl groups) can obviously only produce negative charge.

By combining chemical analyses and titration curves of isolated cell walls of a variety of Gram-positive bacteria, Plette et al. (1995) and Van der Wal et al. (1997a) proposed that carboxylate, phosphate, and amino groups are present roughly in the ratio of 2:1:1. They further report average p*K* values of 4.3, 7.8, and 9.9 for their deprotonation reactions (Plette et al., 1995):

$$\text{R-COOH} \leftrightarrow \text{R-COO}^- + \text{H}^+$$

$$\text{R-PO}_4\text{H} \leftrightarrow \text{R-PO}_4^- + \text{H}^+$$

$$\text{R-NH}_3^+ \leftrightarrow \text{R-NH}_2 + \text{H}^+$$

Cell wall charges predicted by this three-site model are shown in Fig. 7. The model curves in the figure were generated using the constant capacitance model to account for electrostatic effects, while the total functional group (carboxylate + phosphate + amino) concentration was treated as adjustable parameter.

The model curves reproduce the general shape of the pH dependence of the cell wall charge of both bacteria (Fig. 7), with a somewhat higher (cell-normalized) total functional group concentration for *B. subtilis* (9.3×10^{-16} mol cell^{-1}) than for *S. putrefaciens* (6.5×10^{-16} mol cell^{-1}). The model predicted pzc values, however, exceed the measured iep of *S. putrefaciens* by about 0.5 pH units (Fig. 6), in line with the findings of Van der Wal et al. (1997a) for isolated cell walls of five different Gram-positive bacteria. Better agreement between model and data would be possible by adjusting the various model parameters but, without additional constraints, particularly on the pzc and cell wall functional group composition of the bacteria, this represents merely a curve fitting exercise.

The development of cell wall charge is very similar for *S. putrefaciens* and *B. subtilis* (Fig. 7), despite large differences in macromolecular structures of the cell walls. In particular, the more complex cell wall of Gram-negative bacteria is characterized by an outermost layer made up principally of lipopolysaccharides (LPS) (Madigan et al., 1997). A possible explanation is that the LPS layer does not contribute significantly to the charging of the Gram-negative cell wall. This is consistent with the observed low buffering capacity of LPS isolated from *E. coli* (Figs. 4A–C), although it must be kept in mind that the chemical compositions of LPS of *S. putrefaciens* and *E. coli* are different (Jansson, 1999).

5. Conclusions

Time-dependent acid and base consumption curves by live bacterial cells are interpreted to consist of the following three contributions. (1) The near-instantaneous (time scale of minutes) buffer capacity associated with the functional groups present in the cell wall, (2) the short-term (<1 h) utilization of the intracellular buffering capacity, and (3), under basic conditions, the long-term (1–5 h) release of (acidic) metabolic byproducts. By measuring the initial acid or base consumption at different pH values, the passive buffering capacity of the cell wall can thus be determined as a function of the pH of the medium.

The functional group concentrations and the pH dependent cell wall charges inferred from the pH stat experiments for *S. putrefaciens* and *B. subtilis* are in general agreement with those obtained with continuous titrations. Large uncertainties in cell weight (and cell surface areas), however, are currently a major obstacle when comparing results from different research groups. A concerted effort to design standardized procedures to determine these basic cell characteristics would go a long way in generating consistent data sets.

Lipopolysaccharides (LPS), the major constituent of the outermost layer of the cell wall of Gram-negative bacteria, appear to contribute little to the buffer capacity of the intact cell wall. Thus, while LPS may be important in regulating cell adhesion of Gram-negative bacteria, it may not offer many anionic binding sites for metal cations, which must therefore migrate deeper inside the cell wall. The relatively minor buffering capacity associated with LPS may also explain the very similar cell wall charging behavior of Gram-positive and Gram-negative bacteria.

Acknowledgments

The Associate Editor, Johnson R. Haas, and three anonymous reviewers are thanked for their constructive comments and suggestions. This research was financially

supported by the Netherlands Organization for Scientific Research (NWO-Pionier Award).

Associate editor: Johnson R. Haas

References

Agraz, R., van der Wal, A., van Leeuwen, H.P., 1994. Voltrammetric study of the interaction of cadmium with bacterial cells. *Bioelectrochem. Bioenerg.* **34**, 53–59.

Benderitter, M., Vincent-Genod, L., Pouget, J.P., Voisin, P., 2003. The cell membrane as a biosensor of oxidative stress induced by radiation exposure: a multiparameter investigation. *Radiat. Res.* **159**, 471–483.

Borrok, D.M., Fein, J.B., 2005. The impact of ionic strength on the adsorption of protons, Pb, Cd, and Sr onto the surfaces of Gram negative bacteria: testing non-electrostatic, diffuse, and triple-layer models. *J. Colloid Interface Sci.* **286**, 110–126.

Claessens, J., Behrends, T., Van Cappellen, P., 2004. What do acid–base titrations of live bacteria tell us? A preliminary assessment. *Aquat. Sci.* **66**, 19–26.

Cox, J.S., Smith, D.S., Warren, L.A., Ferris, F.G., 1999. Characterizing heterogeneous bacterial surface functional groups using discrete affinity spectra for proton binding. *Environ. Sci. Technol.* **33**, 4514–4521.

Daughney, C.J., Fein, J.B., 1998. The effect of ionic strength on the adsorption of H^+, Cd^{2+}, Pb^{2+} and Cu^{2+} by *Bacillus subtilis* and *Bacillus licheniformis*: a surface complexation model. *J. Colloid Interface Sci.* **198**, 53–77.

Daughney, C.J., Fowle, D.A., Fortin, D., 2001. The effect of growth phase on proton and metal adsorption by *Bacillus subtilis*. *Geochim. Cosmochim. Acta* **65**, 1025–1035.

DiChristina, T.J., 1989. Dissimilative Fe(III) reduction by *Alteromonas putrefaciens* strain 200. Ph.D. Dissertation, California Institue of Technology, Pasadena, CA.

Dzombak, D.A., Morel, F.M.M., 1990. *Surface Complexation Modeling Hydrous Ferric Oxide*. Wiley & Sons, NY.

Fein, J.B., Daughney, C.J., Yee, N., Davis, T.A., 1997. A chemical equilibrium model for metal adsorption onto bacterial surfaces. *Geochim. Cosmochim. Acta* **61**, 3319–3328.

Fein, J.B., Boily, J.-F., Yee, N., Gorman-Lewis, D., Turner, B.F., 2005. Potentiometric titrations of *Bacillus subtilis* cells to low pH and a comparison of modeling approaches. *Geochim Cosmochim Acta* **69**, 1123–1132.

Gelabert, A., Pokrovsky, O.S., Schott, J., Boudou, A., Feurtet-Mazel, A., Mielczarski, J., Mielczarski, E., Mesmer-Dudons, N., Spalla, O., 2004. Study of diatoms/aqueous solution interface. I. Acid–base aquilibria and spectroscopic observation of freshwater and marine species. *Geochim. Cosmochim. Acta* **68**, 4039–4058.

Goncalves, M.L.S., Sigg, L., Reutlinger, M., Stumm, W., 1987. Metal ion binding by biological surfaces: voltrammetric assessment in the presence of bacteria. *Sci. Total Environ.* **60**, 105–119.

Greenstock, C.L., 1981. Redox processes in radiation biology and cancer. *Radiat. Res.* **86**, 196–211.

Haas, J.R., Dichristina, T.J., Wade Jr, R., 2001. Thermodynamics of U(VI) sorption onto *Shewanella putrefaciens*. *Chem. Geol.* **180**, 33–54.

Haas, J.R., 2004. Effects of cultivation conditions on acid–base titration properties of *Shewanella putrefaciens*. *Chem. Geol.* **209**, 67–81.

Jansson, P.E., 1999. The chemistry of O-polysaccharide chains in bacterial lipopolysaccharides. In: Brade, H., Opal, S.M., Vogel, S.N., Morrison, D.C. (Eds.), *Endotoxin in Health and Disease*. Marcel Dekker Inc., New York, pp. 155–178.

Kelly, S.D., Kemner, K.M., Fein, J.B., Fowle, D.A., Boyanov, M.I., Bunker, B.A., Yee, N., 2002. X-ray absorption fine structure determination of pH-dependent U-bacterial cell wall interactions. *Geochim. Cosmochim. Acta* **66**, 3855–3871.

Madigan, T.M., Martinko, J.M., Parker, J., 1997. Biology of Microorganisms. In: Brock, T.D. (Ed.). Prentice Hall International, Inc., New Jersey.

Lovley, D.R., Phillips, E.J.P., 1988. Novel mode of microbial energy metabolism: organic carbon oxidation coupled to dissimilatory reduction of iron or manganese. *Appl. Environ. Microbiol.* **54**, 1472–1480.

Pinchuk, I.V., Bressollier, P., Sorokulova, I.B., Verneuil, B., Urdaci, M.C., 2002. Amicoumacin antibiotic production and genetic diversity of *Bacillus subtilis* strains isolated from different habitats. *Res. Microbiol.* **153**, 269–276.

Plette, A.C.C., van Riemsdijk, W.H., Benedetti, M.F., van der Wal, A., 1995. pH dependent charging behavior of isolated cell walls of a Gram-positive bacterium. *J. Colloid Interface Sci.* **173**, 354–363.

Plette, A.C.C., Benedetti, M.F., van Riemsdijk, W.H., 1996. Competitive binding of protons, calcium, cadmium, and zinc to isolated cell walls of a Gram-positive soil bacterium. *Environ. Sci. Technol.* **30**, 1902–1910.

Prescott, L.M., Harley, J.P., Klein, D.A., 1996. Microbiology, Wm. C. Brown Publishers.

Schultze-Lam, S., Fortin, D., Davis, B.S., Beveridge, T.J., 1996. Mineralization of bacterial surfaces. *Chem. Geol.* **132**, 171–181.

Sokolov, I., Smith, D.S., Henderson, G.S., Gorby, Y.A., Ferris, F.G., 2001. Cell surface electrochemical heterogeneity of the Fe(III)-reducing bacteria *Shewanella putrefaciens*. *Environ. Sci. Technol.* **35**, 341–347.

Urrutia Mera, M., Kemper, M., Doyle, R., Beveridge, T.J., 1992. The membrane-induced proton motive force influences the metal binding ability of *Bacillus subtilis* cell walls. *Appl. Environ. Microbiol.* **58**, 3837–3844.

Van der Wal, A., Norde, W., Zehnder, A.J.B., Lyklema, J., 1997a. Determination of the total charge in the cell walls of Gram-positive bacteria. *Colloids Surf. B Biointerfaces* **9**, 81–100.

Van der Wal, A., Minor, M., Norde, W., Zehnder, A.J.B., Lyklema, J., 1997b. Electrokinetic potential of bacterial cells. *Langmuir* **13**, 165–171.

Venkateswaran, K., Moser, D.P., Dollhopf, M.E., Lies, D.P., Saffarini, D.A., MacGregor, B.J., Ringelberg, D.B., White, D.C., Nishijima, M., Sano, H., Burghardt, J., Stackebrandt, E., Nealson, K.H., 1999. Polyphasic taxonomy of the genus *Shewanella* and description of *Shewanella oneidensis* sp. Nov.. *Int. J. Syst. Biol.* **49**, 705–724.